

# DOSIMETRIC VERIFICATION OF LATERAL PROFILE WITH A UNIQUE IONIZATION CHAMBER IN THERAPEUTIC ION BEAMS

Y. Hara<sup>#</sup>, T. Furukawa, K. Mizushima, R. Tansho, N. Saotome, Y. Saraya, T. Shirai and K. Noda,  
National Institute of Radiological Sciences, Chiba, JAPAN

## Abstract

It is essential to consider large-angle scattered particles in dose calculation models for therapeutic ion beams. However, it is difficult to measure the small dose contribution from large-angle scattered particles. Therefore, we developed a parallel-plate ionization chamber consisting of concentric electrodes (ICCE) to efficiently and easily detect small contributions. The ICCE consists of two successive ICs with a common HV plate. The former is a large plane-parallel IC to measure dose distribution integrated over the whole plane, the latter is a 24-channel parallel-plate IC with concentric electrodes to derive the characteristic parameters describing the lateral beam spread. The aim of this study is to evaluate the performance of the ICCE. By taking advantage of the characteristic of ICCE, we studied the recombination associated with lateral beam profile. Also, we measured a carbon pencil beam in several different media by using ICCE. As a result, we confirmed the ICCE could be used as a useful tool to determine the characterization of the therapeutic ion beams.

## INTRODUCTION

The application of charged particles such as proton and carbon-ion beams for radiotherapy has been increased interest around the world. One solution to make optimal use of therapeutic ion beams and to provide flexible dose delivery is three-dimensional (3D) pencil-beam scanning technique [1-3]. It has been utilized since 2011 at the Heavy Ion Medical Accelerator in Chiba (HIMAC), operated by the National Institute of Radiological Sciences (NIRS) [4]. In the scanning irradiation method, since the 3D dose distribution is achieved by superimposing doses of individually weighted pencil beams determined in the treatment planning, the dose calculation must be more accurate.

In dose calculation, the lateral beam spread due to multiple scattering that elemental pencil beams undergo in matter is generally assumed by a single-Gaussian model. However, the dose contributions from large-angle scattered (LAS) particles are not properly modeled in the single Gaussian. When the field size is too small for scattered particle equilibrium, it has been reported that the single-Gaussian model cannot express the reduction of the doses at the center of the field [5-7]. Therefore, several studies have proposed the expression for pencil beams of the sum of two or three Gaussians [8-11]. The parameterization of LAS particles by the multi-Gaussian model works very well. Generally, it is necessary to

measure the small dose contributions from the LAS particles to derive the parameters. To efficiently and easily measure the small dose contributions, we developed a unique parallel-plate ionization chamber with concentric electrodes (ICCE) [12]. Since the sensitive volume of each channel is increased linearly with radial distance, it is possible to efficiently and easily detect small contributions from the LAS particles.

In this paper, both the measurement using the ICCE and the validity of simplified parameterization of LAS particles are described.

## MATERIALS AND METHODS

### Specification of the ionization chamber with the concentric electrodes

The detailed design of the ICCE was reported previously [12]. Only a simplified explanation is given here. The ICCE consists of two successive ICs with a common HV plate: a large plane-parallel IC to measure dose distribution integrated over the whole plane and a 24-channel parallel-plate IC with concentric electrodes to derive the characteristic parameters describing the lateral beam spread. Figure 1 shows a schematic of measurement system with concentric electrodes. The design of the concentric electrodes is based on the Rayleigh distribution transformed by the bivariate circular Gaussian distribution into polar coordinates. To increase the output at the large off-axis position, we increased the width of the electrode from 0.2 mm to 5.3 mm as a function of radius.

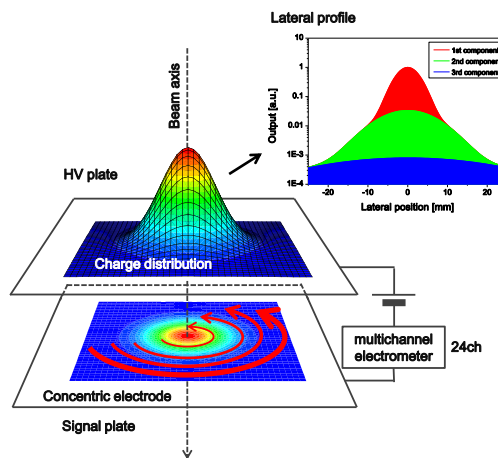


Figure 1: Schematic of the ICCE and lateral profile of carbon-ion expressed by the three-Gaussian model.

The large plane IC should have enough effective area to intercept all particles scattered. The diameter of the chamber is 150 mm. The gap between the HV plate and

<sup>#</sup>y-hara@nirs.go.jp

each signal plate is 2 mm. This chamber is freely open to the atmosphere, where the fill gas is ambient air. Since stray leakage current must be kept to a minimum to preserve accuracy, the signal electrodes were surrounded by annular guard rings.

### Simplified parameterization of LAS particle

The characteristic parameters describing the lateral spreads can be derived from the outputs measured by the ICCE. The measured results can be fitted using three-Rayleigh function that transformed three-Gaussian model into polar coordinates as follows:

$$R(r; \sigma) = \int_{-\pi}^{\pi} \frac{r}{2\pi\sigma^2} \exp\left(-\frac{r^2}{2\sigma^2}\right) d\theta = \frac{r}{\sigma^2} \exp\left(-\frac{r^2}{2\sigma^2}\right),$$

$$F(z, r; t) = \left(1 - \sum_{i=2}^3 f_i(z; t)\right) R_1(r; \sigma_1(z; t)) + \sum_{i=2}^3 (f_i(z; t) R_i(r; \sigma_i)),$$

where  $r$  is the distance from the central point.  $f_i(z; t)$  is the fraction of the integrated dose assigned to the  $i$ -th Rayleigh distribution at a given depth  $z$ , for the range shifter plate of thickness  $t$ .  $R_i$  is the Rayleigh distribution equal to describing the lateral beam spread of the  $i$ -th component with the standard deviation  $\sigma_i$ . Here, we assumed the first component describing three-Rayleigh was dominated by the primary ions. Therefore, lateral beam spread and the fraction of primary ions in the regions beyond the maximum range are set to zero. On the other hand, in the regions beyond the maximum range of primary ions, i.e. in the tail regions, the dose distribution is dominated by dose contribution due to the second and third components. Additionally, the lateral spreads of the second and third components were approximated as invariant with respect to the depth.

### Experimental set up

All experiments were performed with a  $^{12}\text{C}$  pencil beam in the new treatment facility at NIRS-HIMAC, equipped with all the instruments indispensable for 3D scanning irradiation, including a scanning magnet, range shifter, ridge filter and beam monitors [3]. For depth scanning, the hybrid depth scanning method [13] was employed, in which 11 beam energies ranging from 140 MeV/u to 430 MeV/u were used in conjunction with the range shifter.

### Measurement with the ICCE

The ICCE was enclosed in a polymethylmetacrylate (PMMA) waterproof shell so that it could be inserted into the water phantom. The large plane-parallel IC and 24-channel IC were each connected to a Unidos universal dosimeter and two Multidos multichannel dosimeters (both, PTW Freiburg, Germany). The typical high-voltage working value is +1 kV. The ICCE was immersed into a water phantom and scanned in the beam direction by a motor drive. Both the Rayleigh-like dose distribution of the carbon pencil beam and the integrated dose could be

simultaneously measured. Additionally, to verify the reduction of the collected ions due to the general ion recombination, we measured the saturation curves for various applied voltage ranging from +50 V to +1 kV.

### Measurement for the target volume

To prove that three-Gaussian model with the parameters by simplified parameterization adequately describes reality, we measured the lateral dose distributions for the target volume of  $60 \times 60 \times 80 \text{ mm}^3$ . The lateral dose distribution was measured with a pinpoint ionization chamber (PTW31015) which has a sensitive volume of  $0.03 \text{ cm}^3$  connected to a Unidos at the center of a spread-out Bragg peak (SOBP) in water in the horizontal direction from 0 to 100 mm.

### Measurement for different media

To investigate the influence of nuclear reaction caused by  $^{12}\text{C}$  passing through different media, we measured the depth dose distributions and the lateral dose distributions for non-water materials. Non-water materials (water, 40%  $\text{K}_2\text{HPO}_4$ , lard, milk) put into container with thickness of 150 mm is set in front of a water phantom. The ICCE was immersed into a water phantom behind the non-water material. These measurements were repeated at various depths.

## RESULTS AND DISCUSSION

### Saturation curves of ICCE for different electrodes

In Fig. 2, the measured saturation curves are compared with the saturation curves calculated by a calculation model [14] based on the Boag theory [15] for different lateral positions. All calculations could reasonably reproduce the measured distribution. We confirmed the differences of the ion collection efficiency at different lateral positions. This result was attributed to the difference of ionization density dependent on lateral position.

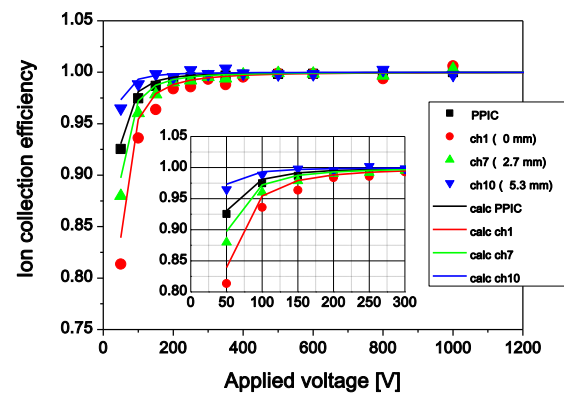


Figure 2: The measured saturation curves (symbols) are compared with the calculated ones (solid lines). PPIC indicates a large plane-parallel IC.

Verification of parameters describing the LAS particles

Figure 3 shows the lateral dose distribution measured by the ICCE at the Bragg peak. The open squares show the fit of the measured results to three-Rayleigh function using the derived parameters of the lateral beam spreads and the fraction factors. The other symbols represent the first, second and third components of the lateral dose distribution fitted by three-Rayleigh function, respectively. In Fig. 4, the depth dose distribution and parameters describing the LAS particles at various depths are shown. As shown in Fig. 4 (b) and (c), while the lateral beam spreads of the second and third components were approximated as invariant with respect to the depth, the fraction factors of the second and third components change steeply from the distal-falloff region to the tail region. Since the fraction of the third component increases as a function of depth, it seems that the third component represents the lighter fragments from a qualitative viewpoint.

To verify the precision of the derived parameters, we calculated the correction factor for the field-size dependence of the doses, “predicted-dose scaling factor” (PDSF) [5, 6]. The PDSF was derived as a ratio of the averaged dose within the target volume optimized with the single-Gaussian form of the pencil beam model to one recalculated with the three-Gaussian model. The dose distribution of 1 Gy was optimized for three target volumes. Figure 5 shows the PDSF for three field sizes. The difference between the PDSF calculated with  $\sigma_2$  and  $\sigma_3$  changed as a function of depth and the one calculated with  $\sigma_2$  and  $\sigma_3$  by approximated as invariant with respect to the depth was 0.1%. As shown in Fig. 6, the calculation using the three-Gaussian model was in good agreement with the measured results. These results show that the simplified parameterization of LAS particles adequately describes the correction for the field-size dependence of the doses.

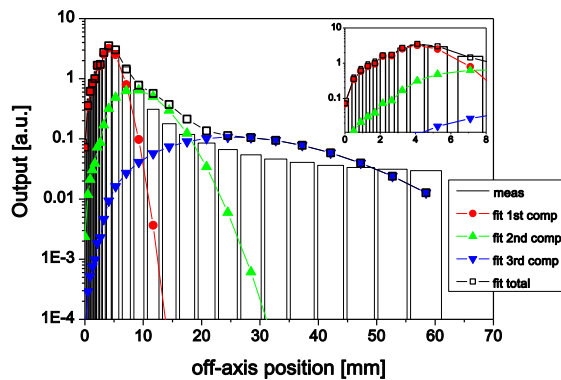


Figure 3: The lateral dose distributions of a 430 MeV/u carbon-ion beam measured at the Bragg peak are shown with the solid line. Each width of the bar charts formed by the solid line represents the widths of the electrodes. Each symbol represents each component of the lateral dose distribution fitted by three-Rayleigh function.

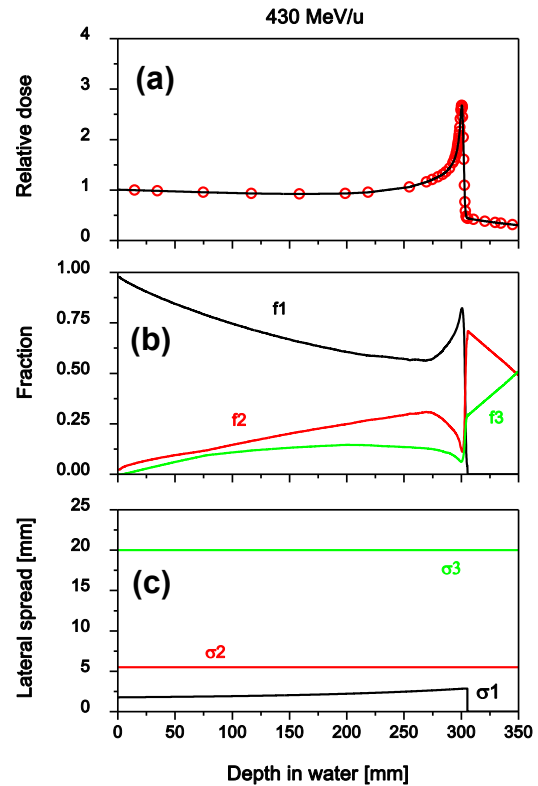


Figure 4: (a) Depth dose distributions measured (open circles) and calculated (solid line). (b) The fraction factors of the first, second and third components fitted by three-Rayleigh function. (c) The lateral beam spreads of the first, second and third components fitted by three-Rayleigh function.

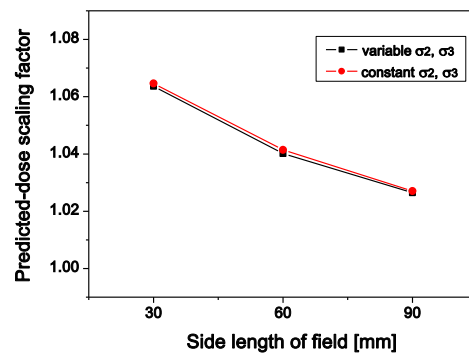


Figure 5: The PDSF for the target volumes of  $30 \times 30 \times 80$ ,  $60 \times 60 \times 80$ ,  $90 \times 90 \times 80$  mm<sup>3</sup>. The closed squares represent the values calculated with  $\sigma_2$  and  $\sigma_3$  changed as a function of depth. The closed circles represent the values calculated with  $\sigma_2$  and  $\sigma_3$  by approximated as invariant with respect to the depth.

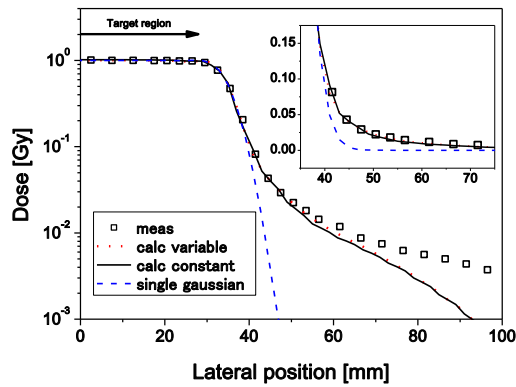


Figure 6: The measured lateral dose distributions (open squares) are compared with those calculated using the three-Gaussian model (solid line) with  $\sigma_2$  and  $\sigma_3$  by approximated as invariant with respect to the depth. For comparison, the calculations using the three-Gaussian model with  $\sigma_2$  and  $\sigma_3$  changed as a function of depth (dotted line) and the calculations using the single-Gaussian model with the PDSF (dashed line) are plotted. The target volume was  $60 \times 60 \times 80 \text{ mm}^3$ .

### Nuclear reaction caused by $^{12}\text{C}$ passing through different media

Figure 7 shows the depth dose distributions for a 400 MeV/u carbon-ion beam measured in water behind non-water material. For milk, the depth dose distribution was almost identical as the one for water. For lard, the Bragg-peak height was 4.5% lower than that for water. This observation suggests that the loss of primary carbon ions in the lard due to nuclear reactions is less than that in water. We also observed a 7.0% increase of the Bragg-peak height for 40%  $\text{K}_2\text{HPO}_4$  compared with that for water. The correction method of the depth dose distribution to account for the dosimetric errors in patient-dose calculations has been reported by Inaniwa et al [16] in detail. As shown in Fig. 8, there is a slight difference between the lateral dose distribution measured in water and those in non-water material. However, these differences are of no clinical significance.

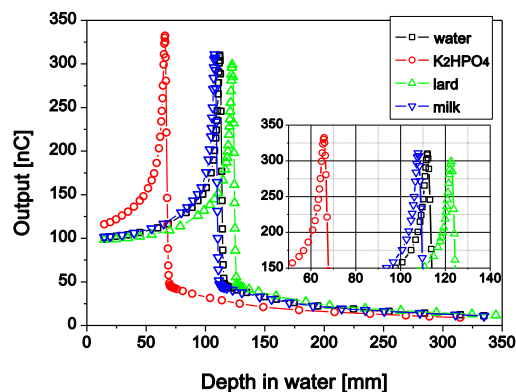


Figure 7: The depth dose distributions measured in water behind non-water material.

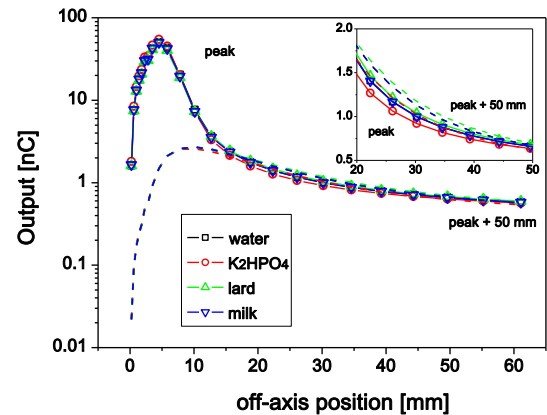


Figure 8: The lateral dose distributions measured in water behind non-water material at Bragg peak (symbols) and peak + 50 mm (dashed lines).

## CONCLUSIONS

We evaluated a unique ionization chamber with concentric electrodes as a useful tool to determine the characterization of the therapeutic ion beams. Simplified parameterization with ICCE makes it possible to easily obtain the parameters describing LAS particles, while maintaining the dose calculation accuracy. Therefore, it will lead to shortened measurements for pencil beam datasets in the commissioning stage. Additionally, it can be easily applied to proton pencil beams. Since it is not necessary to scan the pencil beams, it may also be used for broad-beam delivery systems.

## REFERENCES

- [1] E. Pedroni et al., Med. Phys. 22 (1995) 37.
- [2] Th. Haberer et al., Nucl. Instrum. Methods Phys. Res. A 330 (1993) 296.
- [3] T. Furukawa et al., Med. Phys. 37 (2010) 5672.
- [4] Y. Hirao et al., Nucl. Phys. A 538 (1992) 541.
- [5] E. Pedroni et al., Phys. Med. Biol. 50 (2005) 541.
- [6] T. Inaniwa et al., Med. Phys. 36 (2009) 2889.
- [7] Y. Kusano et al., Med. Phys. 34 (2007) 4016.
- [8] Y. Li et al., Med. Phys. 57 (2012) 983.
- [9] J. Schwaab et al., Phys. Med. Biol. 56 (2011) 7813.
- [10] O. Sawakuchi et al., Phys. Med. Biol. 55 (2010) 3467.
- [11] Y. Kusano et al., Med. Phys. 34 (2007) 193.
- [12] Y. Hara et al., Med. Phys. 41 (2014) 021706.
- [13] T. Inaniwa et al., Med. Phys. 39 (2012) 2820.
- [14] R. Tansho et al., in these proceedings
- [15] J. W. Boag et al., Br. J. Radiol. 23 (1950) 601.
- [16] T. Inaniwa et al., accepted to Phys. Med. Biol.